Evidence for wide scale climate forcing in the late Pleistocene from a speleothem stable isotope record from Spring Valley Caverns, Fillmore County, Minnesota

Daniel Shapiro
Senior Integrative Exercise
March 9, 2007

Submitted in Partial Fulfillment of the Bachelor of Arts Degree from
Carleton College, Northfield, Minnesota

Table of Contents

Evidence for wide scale climate forcing in the late Pleistocene from a speleothem stable isotope record from Spring Valley Caverns, Fillmore County, Minnesota

Daniel Shapiro
Carleton College
Senior Integrative Exercise
March 9, 2007

Advisors:
Clint Cowan, Carleton College
R. Lawrence Edwards, University of Minnesota
E. Calvin Alexander, University of Minnesota

ABSTRACT

Oxygen and carbon stable isotope records from a stalagmite from Spring Valley Caverns, Fillmore County, MN are constrained by U-Th series dating. A continuous growth period between ~62 and ~44 ka indicates that the stalagmite grew throughout the Mid-Wisconsinan interstadial event. Variations in $\delta^{18}O$ indicate that southeastern Minnesota experienced temperature variations of 5.5^{o}C throughout this time. $\delta^{13}C$ values are consistent with spruce charcoal evidence from the Roxana Silt for a conifer forest overlying the karst. Stable isotope profiles from Spring Valley Caverns correlate well with those from other late Pleistocene cave records, including Hulu and Crevice Caves, and with the Greenland ice core records. These correlations are consistent with a large scale climate forcing model.

Keywords: Spring Valley Caverns, Speleothem, Oxygen Isotopes, Carbon Isotopes, Late Pleistocene, Climate Change, Midwestern USA

INTRODUCTION

The identification of past climate patterns and anomalies requires well constrained data from a wide temporal and spatial range. Speleothems are well suited to this task because they record changes in growth conditions over timescales of thousands to hundreds of thousands of years. Speleothems are valuable paleoclimate archives, with the ability to record information regarding climate, vegetation, landscape evolution, and sea level changes, as well as hydrology, nuclide migration, and water rock interactions (Richards and Dorale, 2003).

Among the most widely cited speleothem paleoclimate records is the $\delta^{18}O$ profile generated from a vein calcite from Devil's Hole, Nevada. The Devil's Hole calcite records glacial-interglacial shifts of 1-2 $^{o}/_{oo}$ from 566-60 ka (Winograd et al., 1992). Stalagmites are capable of recording similar variations but at much higher resolutions because of substantially faster growth rates and water residence times of months to years as opposed to kyrs (Dorale and Edwards, 2000). Published stalagmite records (Dorale et al., 1998, Spotl et al., 2002, Wang et al., 2001) have extended the study of regional $\delta^{18}O$ variation and are sufficiently resolved to permit comparison to high resolution data from the Greenland ice cores.

Despite an abundance of caves throughout the Upper Mississipi Valley (Hedges and Alexander, 1985), few studies have attempted to use speleothems to record climatic conditions in the beginning of the last glacial period (Lively, 1983, and Dorale et al., 1998). This study uses Uranium-Thorium dating to constrain growth periods for a stalagmite, designated SVC-06, from Spring Valley Caverns, Minnesota, and to provide a timescale for the comparison of stable isotope data from SVC-06 to other records. These

comparisons can be used to identify climate patterns and vegetation changes, and to evaluate local landscape evolution.

SPELEOTHEMS

Formation

Speleothems are cave mineral bodies formed by chemical precipitation from flowing or dripping groundwater. Calcite is the dominant mineral precipitated, although aragonite, gypsum, and other evaporite deposits are common (Ford and Williams, 1983). Calcite speleothems are formed by degassing of CO_2 from supersaturated groundwater. Speleothems take on a number of different forms, including stalactites, draperies, stalagmites, flowstones, cave pearls, and moonmilk.

The process of speleothem formation begins when rain water becomes acidic as it moves through the soil horizon. This water then dissolves carbonate bedrock, quickly becoming saturated with respect to $CaCO_3$. Caves form when this water interacts with groundwater of a higher pCO_2 to produce a mixing zone undersaturated with respected to $CaCO_3$. If groundwater encounters an air filled cavity with lower pCO_2, such as a cave, the water will degas, prompting carbonate deposition.

Suitability for Paleoclimate Reconstruction

The extreme fractionation of Uranium parent isotopes (^{238}U, ^{235}U, and ^{234}U, from their daughter isotopes (^{230}Th and ^{231}Pa) allow the dating of speleothems using either Uranium-Thorium or Uranium Protactinium dating series (Langmuir, 1997; Dorale *et al.*,

2001). This provides a temporal framework for paleoclimate analysis, and allows definite association of observed climate trends with signals from other locations.

Speleothems are archives of secondary information that can be used to gain insight into their overlying environments (Richards and Dorale, 2003). Yonge et al. (1985) showed in a study of caves throughout North America that the stable isotope content of drip water feeding speleothems is invariant on yearly timescales. Seasonal differences in the stable isotope content of precipitation are homogenized as groundwater flows through the karst, and therefore the $\delta^{18}O$ composition of the stalagmite is representative of the $\delta^{18}O$ content of precipitation over one to several years. Dansgaard (1964) found that the $\delta^{18}O$ of modern mean annual precipitation (MAP) at the midlatitudes is predominantly a function of mean annual temperature (MAT). The relationship between $\delta^{18}O$ of MAP and MAT is empirically ~0.6 per mil/^{o}C. Because of this relationship speleothems have excellent potential as subjects for study of long-term temperature trends.

Speleothem $\delta^{13}C$ values reflect overlying vegetation because drip waters pass through overlying soil. The carbon isotope composition of soil organic content is determined by the vegetation present (Dorale et al., 1998). Variations in $\delta^{13}C$ of soil organic matter reflect the different photosynthetic pathways of C_3 and C_4 plants (Boutton, 1991). C_3 plants include most trees and cool season grasses and are more abundant in cool moist climates. C_4 plants are dominantly warm season grasses and are prevalent in warm arid settings (Denniston et al., 1999). C_4 plants have a higher $\delta^{13}C$ than C_3 plants (from -19 to -9 per mil for C_4, compared to -32 to -20 per mil for C_3) and this signal is preserved as drip water makes its way from the surface to the cave environment (Dorale

et al., 1998). Speleothem $\delta^{13}C$ can therefore be used to determine whether forests (expected speleothem $\delta^{13}C$ from -14 to -6 per mil) or grasslands (expected speleothem $\delta^{13}C$ greater than -6 per mil) dominated the ecosystem. Atmospheric CO_2 is thought to have negligible input into the speleothem $\delta^{13}C$ signal (Baker et al, 2002).

PREVIOUS STUDIES FROM THE UPPER MISSISSIPPI VALLEY

Hedges and Alexander (1985) provide a summary of the karst-related features of the Upper Mississippi Valley. They identify the region as having a wide variety of cave and karst systems, ranging in age from Ordovician to Tertiary, and encompassing types such as maze caves, interstratal caves, hydrothermal caves, stream piracy caves, soil piping pseudokarsts, and periglacial parakarsts, among others.

Despite the abundance of caves of various ages in the Upper Mississippi Valley, most paleoclimate studies have focused on Holocene age reconstructions. Denniston *et al.* (1999) and Baker *et al.* (2002) used speleothems from 4 caves, including Spring Valley Caverns, to document climate shifts over the past 8000 kyr. They use $\delta^{13}C$ data from stalagmites from the 4 caves to determine the arrival of prairie at cave locations throughout the Holocene. From the relatively stable position of the prairie-forest ecotone they inferred that the boundary was determined by a moisture gradient due to the encroachment of Pacific air into the Upper Mississippi Valley, decreasing available moisture during the growing season (Denniston *et al.,* 1999).

Lively (1983) used U-series dating on speleothems from Mystery Cave in southeastern Minnesota to determine the extent of glaciation throughout the late Quaternary in the Upper Mississippi Valley. He identifies 3 periods of speleothem

growth in the last 170,000 kyr; from 170,000 to 90,000 yr. B.P., from 70,000 to 35,000 yr. B.P., and from 13,000 yr B.P. to the present. These growth periods correspond to the end of the Illinoisan glaciation and the following Sangamon interstadial, a mid Wisconsinan interstadial, and relatively warm conditions after the termination of the Wisconsin glaciation.

Dorale *et al.* (1998) use stalagmite records from Crevice Cave, Missouri to generate a paleoclimate and paleovegetation history from 75 to 25 kyr. Oscillations in $\delta^{13}C$ are interpreted as transitions between grassland and forest environments, with grassland dominating from 71-55 kyr and forests from 55-25 kyr. Ranges in $\delta^{18}O$ of ~1.4 per mil are interpreted as reflecting changes in mean annual temperature of approximately $4^{o}C$ over the life of the stalagmite. Frequent $\delta^{18}O$ oscillations in the Crevice Cave record suggest warm/cool cycles on the order of 3000 to 7000 years. This frequency suggests that the speleothems record Heinrich events and Dansgaard-Oeschger cycles (Bond et al., 1993).

GEOLOGICAL SETTING

Spring Valley Caverns (SVC, $43^{o}44'24"$ N, $92^{o}24'36"$ W), Fillmore County, MN, are developed in the Stewartville Dolostone of the Upper Ordovician Galena Group (Denniston *et al.*, 1999, Runkel et al., 2003, Fig. 1). The caverns are developed under a local topographic high adjacent to incised valleys, and are approximately 30 m below the surface (Denniston et al., 1999). Spring Valley Caverns are classified as a water-inlet maze cave, which serve hydraulically to carry surface water to an aquifer (Runkel et al., 2003)

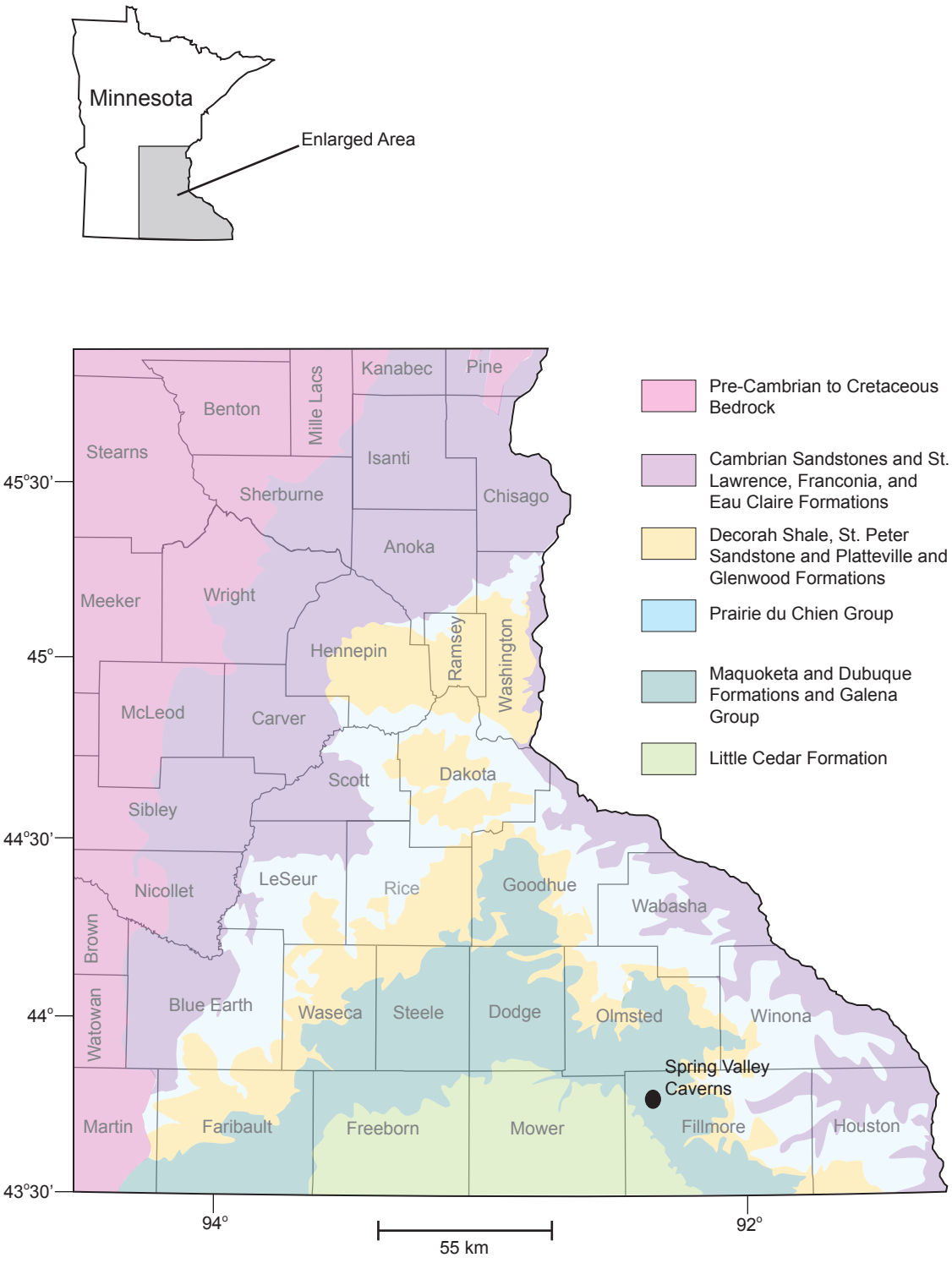

Figure 1. Simplified Geological Map of Southeastern Minnesota showing location of Spring Valley Caverns (43°44'24" N, 92°24'36" W) in Fillmore County. Spring Valley Caverns is formed in the Stewartville Dolostone of the Galena Group (Denniston et al. 1999). Map adapted from Runkel et al. (2003).

The Stewartville Formation has high porosity, and the large number of sinkholes and caves that have developed in the unit suggest that it may be particularly susceptible to the development of large, interconnected pore networks (Runkel et al., 2003). Spring Valley Caverns is an extensive cave system consisting of more than 5 miles of traversable passages (Fig. 2). Sample SVC-06 is a stalagmite that was found broken at the base by the cave owner several hundred feet from cave entrance SVC I in the summer of 2006.

URANIUM-SERIES DATING

Any material that (1) contains measurable Uranium, (2) has negligible Thorium, and (3) remains a closed system, is datable by U-Th techniques; speleothems are one of the few natural materials which satisfy all three criteria (Dorale et al., 2001). Uranium-series dating of speleothems is possible because of the different solubilities of U and Th. Uranium is highly mobile in the hydrosphere as the soluble UO_2^{2+} (uranyl ion) and is frequently found in various uranyl carbonate complexes (Richards and Dorale, 2003). Thorium, meanwhile, is found in a +4 oxidized state and has an extremely low solubility (Langmuir, 1980). Waters feeding secondary calcite and aragonite deposits can therefore be expected to contain a negligible Th concentration and a relative abundance of U, which is reflected in the deposit (Richards and Dorale, 2003).

Because initial Th concentrations in speleothem carbonate are negligible, any measured Thorium can be assumed to have formed as a result of the radioactive decay of Uranium. Activity, or decays per unit time, (dN/dT) is equal to $N\lambda$, where N is t he number of atoms and λ is the decay constant for that nuclide, and T is time. The half life of a nuclide is defined as $(\ln 2)/ \lambda$. ^{234}U and ^{230}Th are the longest lived intermediate

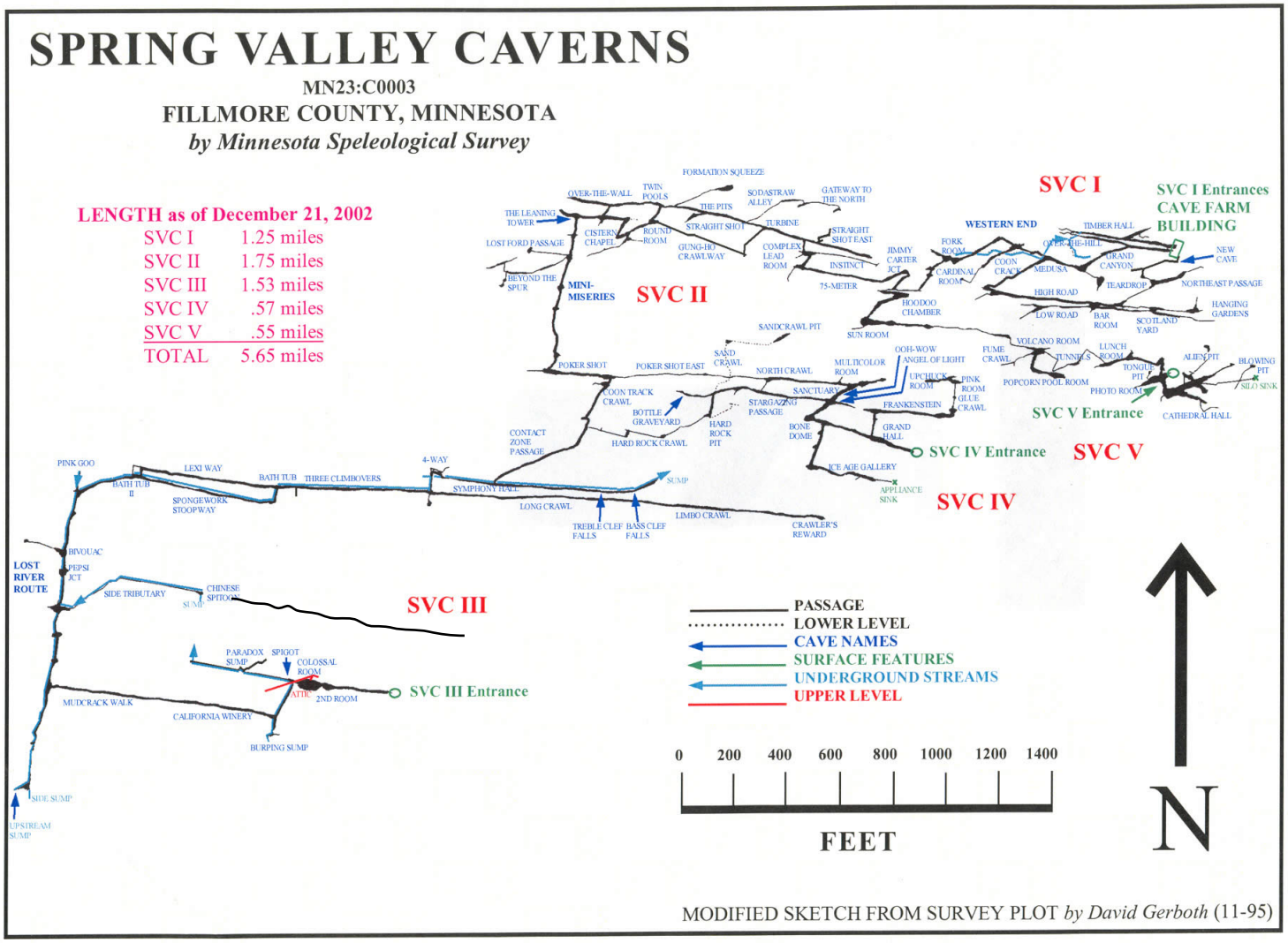

Figure 2. Map of Spring Valley Caverns. Stalagmite SVC-06 was found broken by the cave owner several hundred feet from the entrance to SVC I (upper right), and placed near the entrance for collection. Map courtesy of the Minnesota Speleological Survey.

daughters of the ^{238}U - ^{206}Pb decay series (Dorale *et al.*, 2001). That series with only the relevant nuclides and their half lives is:

$$^{238}U \rightarrow {}^{234}U \rightarrow {}^{230}Th \rightarrow {}^{206}Pb$$

$$4.468 \times 10^{9}\ y \qquad 2.453 \times 10^{5}\ y \qquad 7.569 \times 10^{4}\ y$$

If the crystal lattice of the speleothem remains closed after formation then any U lost as a result of radioactive decay will result in Th gain. The equation for radioactive production and decay of ^{238}U, ^{234}U, and ^{230}Th is:

$$[^{230}Th/^{238}U] = 1 - e^{-\lambda 230 T} + (\delta^{234}U_{(m)}/1000)\ (\lambda_{230}/\{\lambda_{230} - \lambda_{234}\})\ (1 - e^{(\lambda 234 - \lambda 230)T})$$

(modified from Kaufman and Broecker, 1965 by Dorale et al., 2001),

where the λ's represent decay constants, $[^{230}Th/^{238}U]$ denotes the $^{230}Th/^{238}U$ activity ratio, $\delta^{234}U_{(m)} = ([^{234}U/^{238}U] - 1)*1000$ and T is age. Age can be calculated using the above equation if $\delta^{234}U$ and $[^{230}Th/^{238}U]$ can be measured and the decay constants are known.

SAMPLING/DATA COLLECTION

Uranium Series Dating

The stalagmite was sawn in half vertically and polished prior to sampling. Samples for dating were obtained by milling along the central axis using a hand held dental drill and a 1.0 mm carbide burr. An effort was made to take samples only from unaltered calcite. In the case of SVC-06, unaltered calcite is a translucent yellow that is interpreted as optically continuous (Ford and Williams, 1989, Kral 1971). Samples were

obtained by scraping off the resulting powdered material onto weigh paper and then into a pre-weighed polyethylene vial. Sample sizes ranged from approximately 80-100 mg.

Procedures for chemical separation are similar to those described by Edwards et al. (1987) for corals but involve smaller reagent volumes due to the reduced sample sizes. Samples were transferred to pre-weighed 30 ml Teflon vials and reweighed. Samples were covered with approximately 5 ml deionized water and dissolved by dropwise addition of 14N HNO_3. Samples were then spiked with a mixed ^{229}Th-^{233}U solution of known concentration and isotopic composition. Organics were destroyed by refluxing the dissolved sample with 3-5 drops of $HClO_4$, and the samples were then dried on the hotplate. While still hot the samples were redissolved in 1N HCl and 1 drop of $FeCl_2$ was added. U and Th were co-precipitated with Fe by the dropwise addition of NH_4OH. The precipitate was rinsed 3 times, dissolved in 14N HNO_3, dried, and dissolved an additional 2 times in 14N HNO_3. Samples were then transferred to 0.5 ml anion exchange columns (SPECTRUM Spectra Gel Ion Exchange 1X8, chloride form, particle size 75-150 μm). Iron was removed by washing with 1.5 column volumes of 7N HNO_3, Thorium by 4 column volumes of 8N HCl, and Uranium by 4 column volumes of water. Uranium and Thorium subsamples were then dried down and dissolved in a weak nitric acid solution in preparation for analysis.

Dating was carried out at the Minnesota Isotope Laboratory using inductively coupled mass spectrometry (ICP-MS). Analyses were made using a Finnigan-MAT Element with a double focusing sector-field magnet in reversed Nier-Johnson geometry. New Brunswick Laboratoy Certified Reference Material 112A (NBL-112A, formerly National Bureau of Standards Reference Material 960), a Uranium standard, was run

daily to correct for error introduced by multiplier intensity bias and to correct for peak shift. A Cetac Aridus II nebulization system was used for most samples to eliminate contamination from previous samples. In instances where the Aridus was not used this contamination was prevented by cleaning the nebulization chamber with dilute HNO_3 + HF and by running dilute HNO_3 + HF through the system prior to introducing the next sample. Measurement times were approximately 20 minutes for U and 10 minutes for Th, corresponding to approximately 8000 sets of U data and 2000 sets of Th data.

Stable Isotope Analyses

Linear interpolation of U-series dates was used to determine sampling frequency for dated intervals such that sampling resolution was ~200 years. Approximately 30 μg of powdered sample was collected from along the central axis of the stalagmite by means of a hand held dental drill using a 0.7 mm carbide dental burr. Samples were analyzed at the Paleoenvironment and Neotectonics Laboratory at the National University of Taiwan.

RESULTS AND DISCUSSION

U-Series Dates

Dates from 16 sites along the stalagmite show continuous growth throughout the life of the formation (Table 1, Figure 3). Samples SVC06-03-1 and SVC-06-03-2, milled from the same location on the stalagmite, are within error; SVC-06-03-2 is used in further analysis because of its smaller analytical error. Samples are in stratigraphic order, within error, except for SVC-06-13 and SVC-06-10. SVC-06-4 shows a reversal within error, and is not used in growth rate calculations. Sample SVC-06-10 was milled from a visibly

Table 1. Uranium and thorium isotopic compositons and 230Th ages for Stalagmite SVC-06, from Spring Valley Caverns
Analytical errors are 2σ of the mean.

Depth mm	Sample ID	Sample Size (g)	^{238}U ppb	$\delta^{234}U$ measured[a]	$[^{230}Th/^{238}U]$ activity[c]	$[^{230}Th/^{232}Th]$ ppm[d]	Age corrected [c,e]
6	SVC-06-01	0.1039	860.0 ± 1.2	774.8 ± 2.0	0.60582 ± 0.00231	171375 ± 152496	44,146 ± 210
35	SVC-06-14	0.0916	2384.8 ± 4.2	766.5 ± 3.4	0.63281 ± 0.00253	86701 ± 15290	46,792 ± 253
69	SVC-06-03-1	0.0726	3015.1 ± 5.8	704.1 ± 2.4	0.64656 ± 0.00850	61465 ± 7582	50,268 ± 817
69	SVC-06-03-2	0.0971	3001.1 ± 7.1	708.0 ± 3.1	0.64302 ± 0.00359	58396 ± 5130	49,786 ± 360
99	SVC-06-13	0.0766	8100.8 ± 17.6	575.8 ± 2.6	0.68331 ± 0.00392	490996 ± 159856	59,700 ± 458
99	SVC-06-15	0.1132	4555.5 ± 10.3	647.5 ± 3.5	0.62979 ± 0.00267	43819 ± 1677	50,818 ± 300
130	SVC-06-08	0.0834	4626.5 ± 10.6	637.6 ± 2.8	0.63546 ± 0.00405	81441 ± 7634	51,786 ± 424
163	SVC-06-16	0.0903	4511.0 ± 9.7	606.9 ± 3.2	0.63117 ± 0.00270	39043 ± 1679	52,624 ± 310
267	SVC-06-17	0.0911	4295.4 ± 10.2	591.5 ± 3.6	0.65439 ± 0.00310	533141 ± 312017	55,760 ± 373
303	SVC-06-07	0.0812	3799.3 ± 10.2	680.9 ± 3.6	0.70431 ± 0.00440	21459 ± 618	56,920 ± 477
336	SVC-06-12	0.0872	5280.5 ± 10.8	536.6 ± 2.4	0.65257 ± 0.00279	343627 ± 110468	58,222 ± 342
364	SVC-06-11	0.0990	3475.2 ± 6.7	665.6 ± 2.6	0.71445 ± 0.00406	273444 ± 85530	58,677 ± 442
388	SVC-06-10	0.0838	2948.1 ± 7.1	646.5 ± 3.5	0.63188 ± 0.00285	25492 ± 1177	51,062 ± 317
410	SVC-06-09	0.0928	4135.9 ± 9.0	637.4 ± 2.9	0.70794 ± 0.00332	143299 ± 21258	59,334 ± 382
446	SVC-06-06	0.0775	2803.6 ± 6.1	681.5 ± 2.9	0.74091 ± 0.00364	121083 ± 25609	60,695 ± 408
526	SVC-06-05	0.0822	3043.0 ± 6.1	692.6 ± 2.4	0.76227 ± 0.00347	222858 ± 73225	62,400 ± 387
533	SVC-06-04	0.0818	4255.6 ± 8.3	567.9 ± 2.2	0.70549 ± 0.00368	599406 ± 411222	62,641 ± 442
588	SVC-06-02	0.1063	2642.2 ± 9.1	492 ± 2.2	0.66956 ± 0.00306	46429 ± 3228	62,635 ± 395

[a] $\delta^{234}U = ([^{234}U/^{238}U]_{activity} - 1) \times 1000$.

[b] $\delta^{234}U_{initial}$ corrected was calculated based on ^{230}Th age (T), i.e., $\delta^{234}U_{initial} = \delta^{234}U_{measured} \, X \, e^{\lambda 234 * T}$, and T is corrected age.

[c] $[^{230}Th/^{238}U]_{activity} = 1 - e^{-\lambda_{230} T} + (\delta^{234}U_{measured}/1000)[\lambda_{230}/(\lambda_{230} - \lambda_{234})](1 - e^{-(\lambda_{230} - \lambda_{234}) T})$, where T is the age.

Decay constants are 9.1577×10^{-6} yr^{-1} for ^{230}Th, 2.8263×10^{-6} yr^{-1} for ^{234}U, and 1.55125×10^{-10} yr^{-1} for ^{238}U (Cheng et al., 2000).

[d] The degree of detrital ^{230}Th contamination is indicated by the $[^{230}Th/^{232}Th]$ atomic ratio instead of the activity ratio.

[e] Age corrections were calculated using an average crustal $^{230}Th/^{232}Th$ atomic ratio of $4.4 \times 10^{-6} \pm 2.2 \times 10^{-6}$.

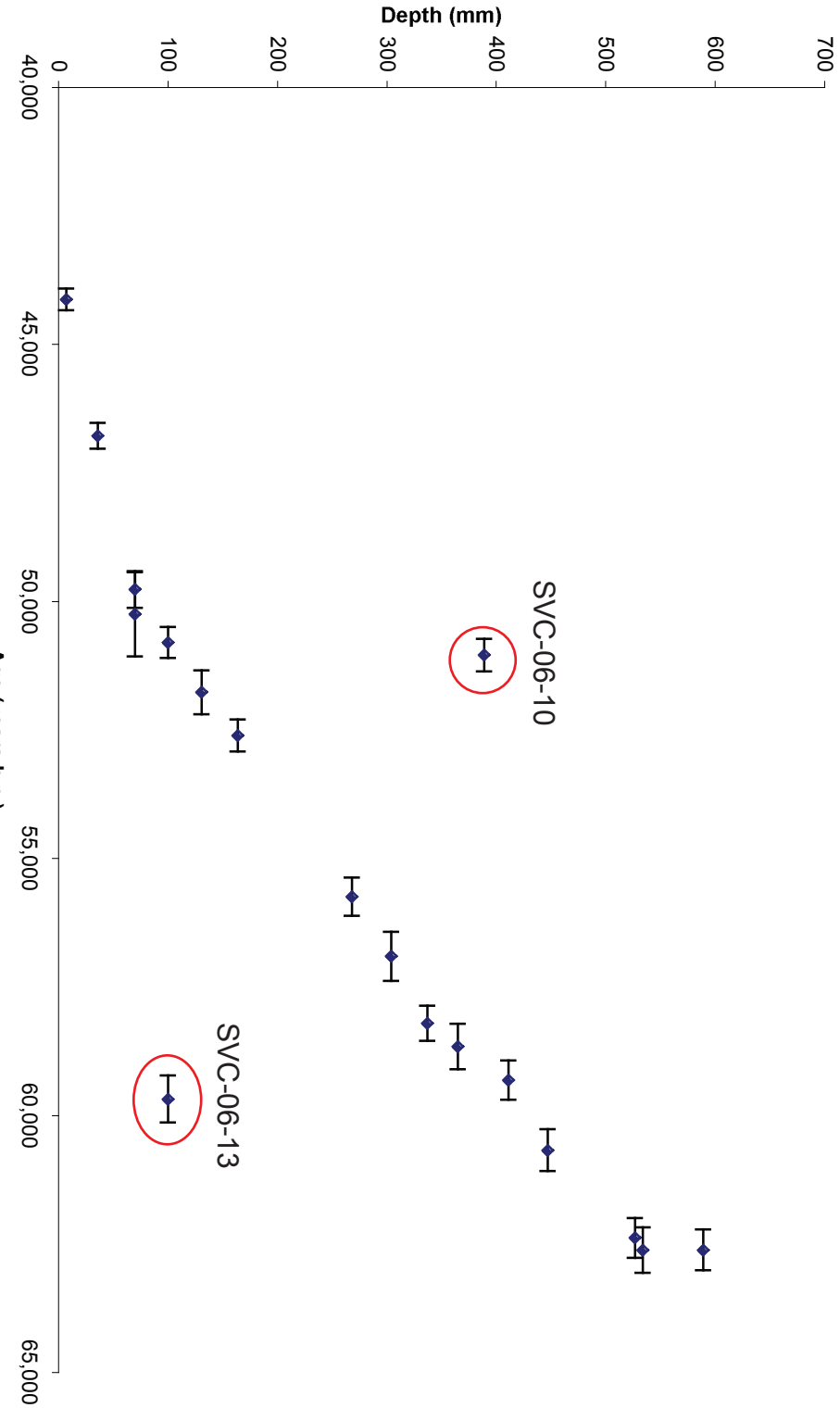

Figure 3. Age vs. Depth for Stalagmite SVC-06. The two circled points are out of order stratigraphically and are discussed in the text. Other points show continuous growth over the life of the stalagmite.

porous area of the stalagmite, and is interpreted to have been altered by post depositional fluid flow. Any new material deposited from this flow into pore space would result in a younger measured age at this location then is predicted by stratigraphy. The date measured at site SVC-06-10 is therefore not included in further analyses. The deviation from stratigraphic order observed in sample SVC-06-13 is interpreted to have resulted from contamination from an older sample run previous to SVC-06-13. Sample SVC-06-15 is from the same location as SVC-06-13, and shows a measured age in correct stratigraphic order. Therefore further analyses use the date determined by SVC-06-15.

Growth occurred from 62,639 kyr – 44,146 kyr. A general slowing of growth rate is observed over the life of the stalagmite, ranging from an initial rate of ~.26 mm/yr to a rate of ~.011 mm/yr in the final stages of growth (Fig. 4). This period of growth corresponds well with the Mid-Wisconsinan interstadial which occurred in the Midwest between 30,000 and 70,000 yr B.P., and was recognized in geological mapping carried out by Frye and Willman (1973) and by Dreimanis and Goldthwait (1973). This interstadial was also recognized by Lively (1983) in speleothems from Mystery Cave and other surrounding caves in southern Minnesota.

The Mid-Wisconsinan interstadial was a period marked by moderation in climate in comparison to the glacial periods that surrounded it. Speleothem formation is rare in caves beneath glacial ice (see Ford *et al.*, 1983 and Atkinson, 1983 for treatment), and it is accepted that speleothem formation will halt when the karst surface is covered by ice or permafrost (Spötl et al., 2002). Spring Valley Caverns lies on the margin of the "driftless area" suggested by Lively (1983, Fig. 5), which is thought to have remained free of ice throughout the Wisconsinan Glaciation (Fry and Willman, 1973). Continuous

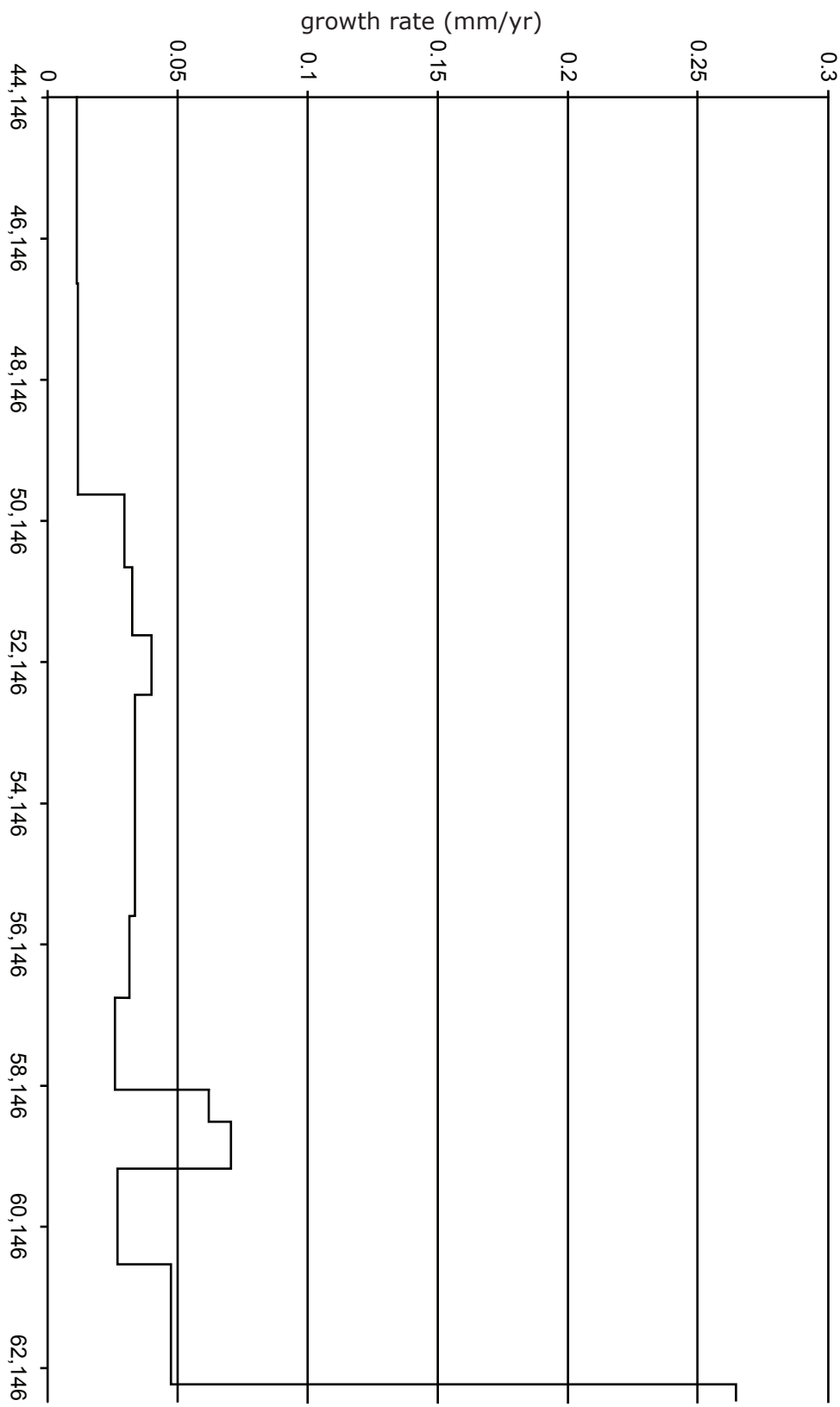

Figure 4. Growth Rate of stalagmite SVC-06 plotted over time., showing trend of decreasing growth rate over time. Growth rates were calculated using linear interpolation between points.

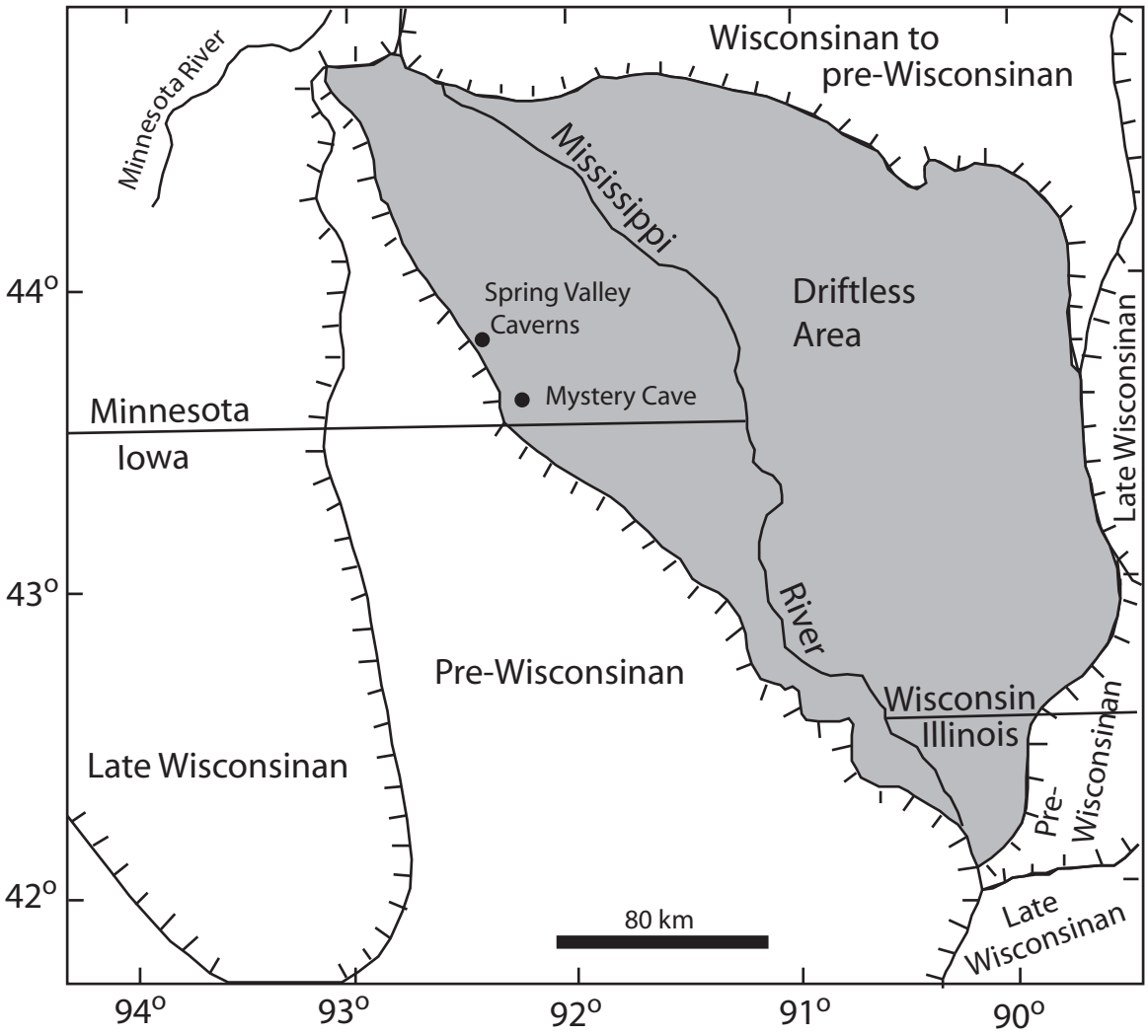

Figure 5. Locations of Spring Valley Caverns and Mystery Cave relative to the Driftless Area of the Upper Mississippi Valley. The Driftless Area was ice free throughout the last glaciation. Map adapted from Runkel (1983).

growth throughout the life of the stalagmite suggests that the retreat of permafrost at the onset of the interstadial and the advancement of permafrost at the termination of the interstadial constrained periods of growth at SVC. Thus the onset of growth corresponds with ice free conditions over SVC and termination of growth represents the advancement of permafrost over the karst, concurrent with reinvigorated glaciation.

Stable Isotope Analyses

$\delta^{13}C$ and $\delta^{18}O$ curves are presented in figure 6. Because evaporative processes can cause additional fractionation of Oxygen isotope species, it is necessary to constrain kinematic fractionation before making paleoclimatic inferences from speleothem records (Hendy and Wilson, 1968). Kinetic fractionation can be tested for by checking for covariance between $\delta^{13}C$ and $\delta^{18}O$ values (Fig. 7). The low R^2 value indicates that no kinematic fractionation occurred and supports equilibrium deposition.

The $\delta^{18}O$ record for SVC-06 ranges from a high of ~-2.8 per mil to a low of ~4.7 per mil. Fractionation of -.26 per mil/^{o}C between calcite and water counteracts the initial 0.6 per mil/^{o}C $\delta^{18}O$ of MAP to MAT relationship, resulting in a net fractionation relationship of approximately 0.35 per mil/^{o}C (Friedman et al., 1977 and Dorale et al., 1998). Thus, the ~1.9 per mil range in the SVC-06 $\delta^{18}O$ record represents a MAT range of approximately 5.5^{o}. The warmest temperatures are observed at around 62 ka and the coldest temperatures are found around 53 ka. The $\delta^{13}C$ records range from a high of ~-6.25 per mil at 62.5 ka to a low of ~-8.85 per mil at ~52 ka.

Similarities in the $\delta^{18}O$ profiles of SVC, Crevice Cave, Missouri and Spring Valley Caverns and an antiphased relationship between a record from Hulu Cave, China

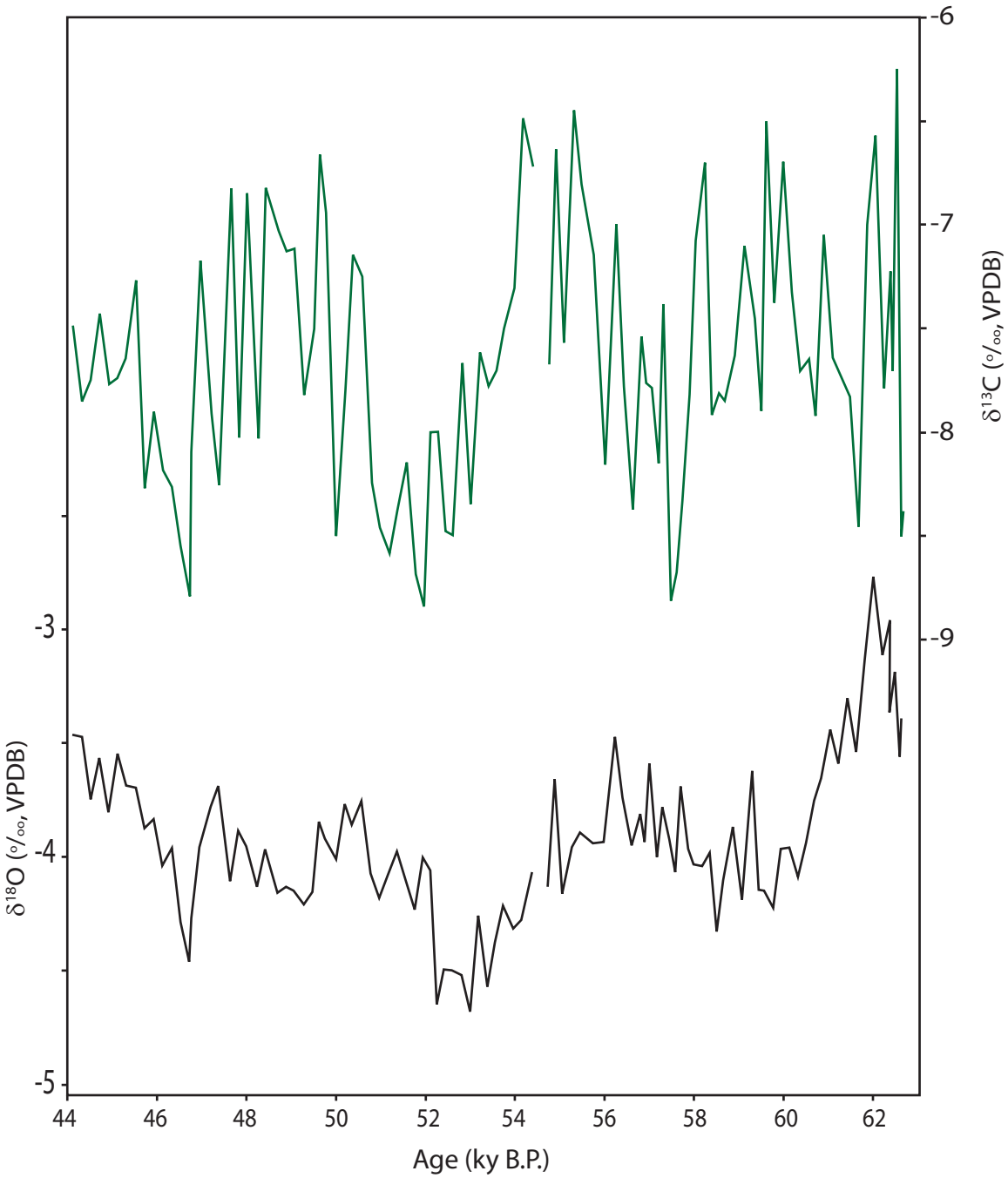

Figure 6. Carbon $\delta^{13}C$ (green) and Oxygen $\delta^{18}O$ (black) profiles for SVC-06.

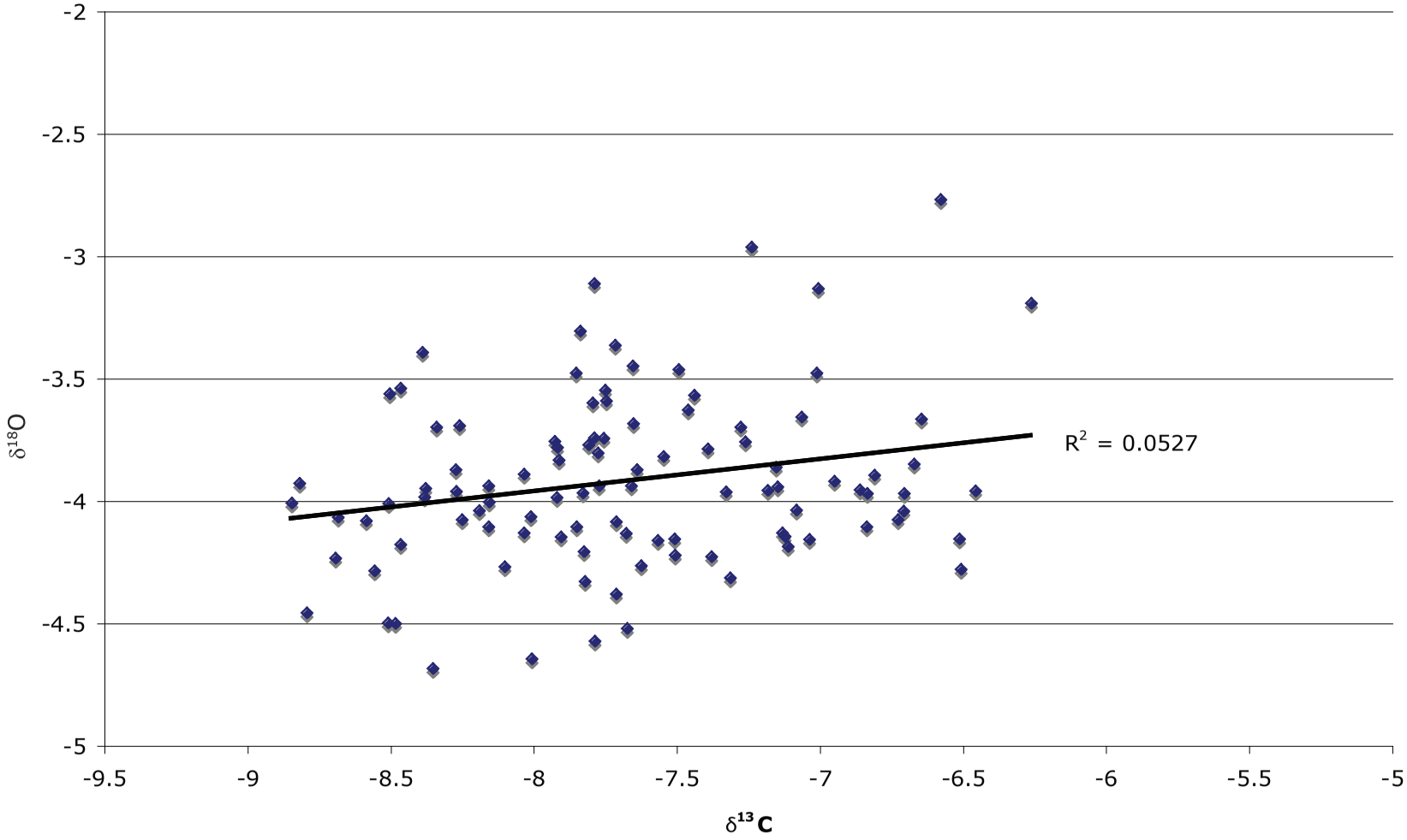

Figure 7. Carbon $\delta^{13}C$ vs. Oxygen $\delta^{18}O$ for stable isotope samples from SVC-06. Low R^2 value indicates no covariance between the two datasets and supports equilibrium fractionation during formation of the stalagmite.

and Spring Valley support a large scale causal mechanism for climatic variations observed over the mid-Wisconsinan interstadial (Fig. 8). Figure 9 shows the broad similarities between the $\delta^{18}O$ records from SVC and two Greenland ice core records, the Greenland Ice-Core Project (GRIP), and the Greenland Ice Sheet Project 2 (GISP2). Dansgaard-Oeschger events (D-O events), warm periods of 1-3 kyr duration which occurred throughout the last glacial period (Dansgaard et al., 1993), are readily identifiable in the SVC $\delta^{18}O$ curve and can be correlated to the Greenland cores. Cooling trends are less easily identifiable in the SVC profile than in those of the ice cores, especially that between D-O events 14 and 13.

MODEL FOR LATE PLEISTOCENE CLIMATE

Possibly analogous to D-O cycles, and more extensively studied, are the Bölling (warming) and Youger-Dryas (YD, cooling) oscillations that occurred during the last glacial termination (~15-11 kyr). These events are well recorded in Greenland by Alley et al. (1993) and in Europe by Björck et al. (1996), who estimated cooling of ~10^{o}C for YD events. North American evidence for YD cooling comes from sites along the Atlantic coast (Kneller and Peteet, 1999), and suggests that a change in North Atlantic Deep Water (NADW) circulation was responsible for the YD cold reversal (Broecker, 1994).

Broecker (1994) and Björck et al. (1996) have postulated that glacial rafting and melting in response to warm temperatures could inject large quantities of freshwater into the northern Atlantic, disrupting thermohaline circulation. This is supported by high percentages of lithic fragments found in ocean sediments deposited in Heinrich layers,

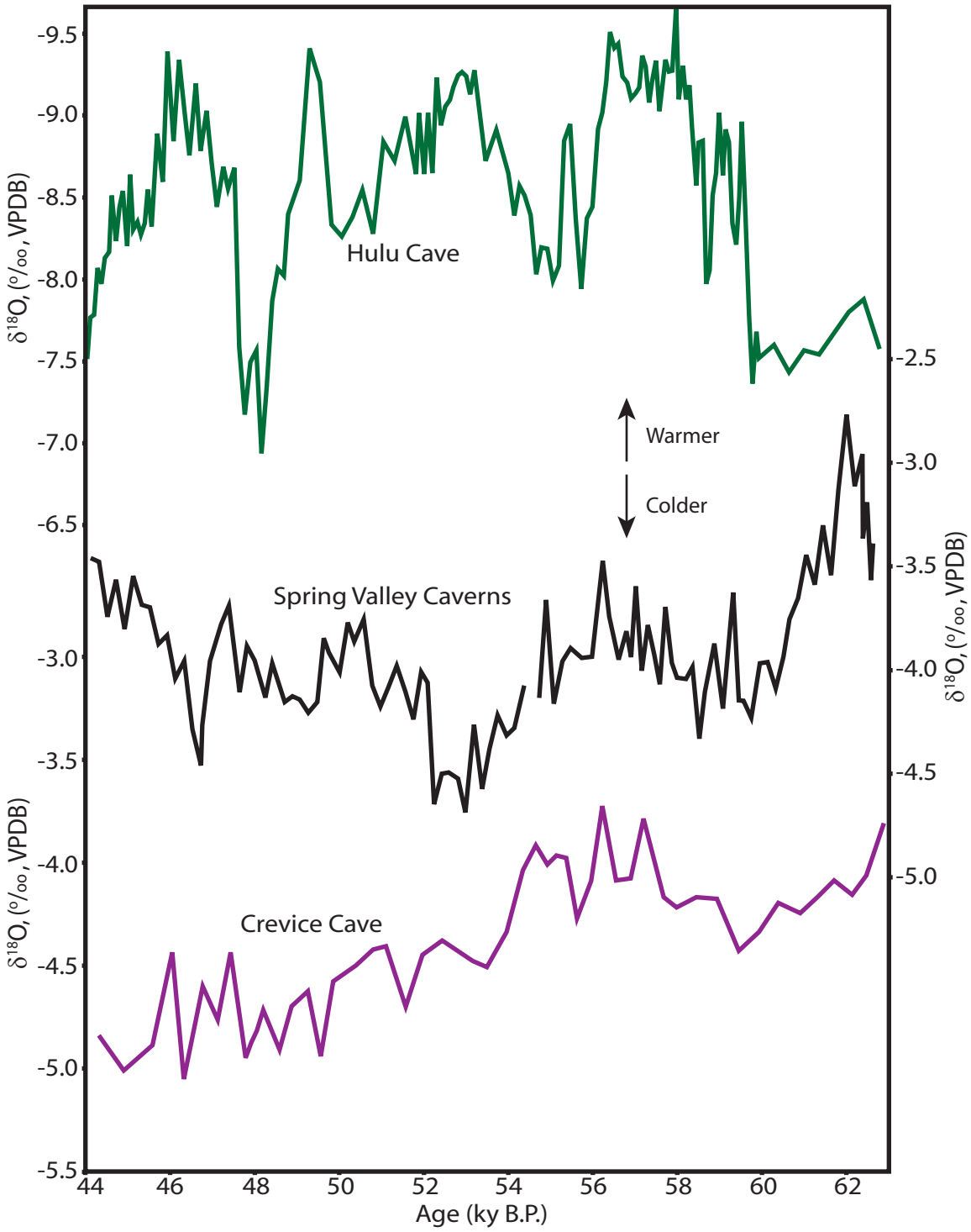

Figure 8. Spring Valley Caverns $\delta^{18}O$ record compared to contemporaneous records from Hulu Cave, China, and Crevice Cave, Missouri. The Hulu Cave record scale is inverted because the stable isotope content of precipitation at that site is controlled by the amount effect (Wang et al., 2001). Crevice Cave and Spring Valley records are correlable, while Hulu is antiphased with the Spring Valley record, indicating hemispheric scale climate forcing.

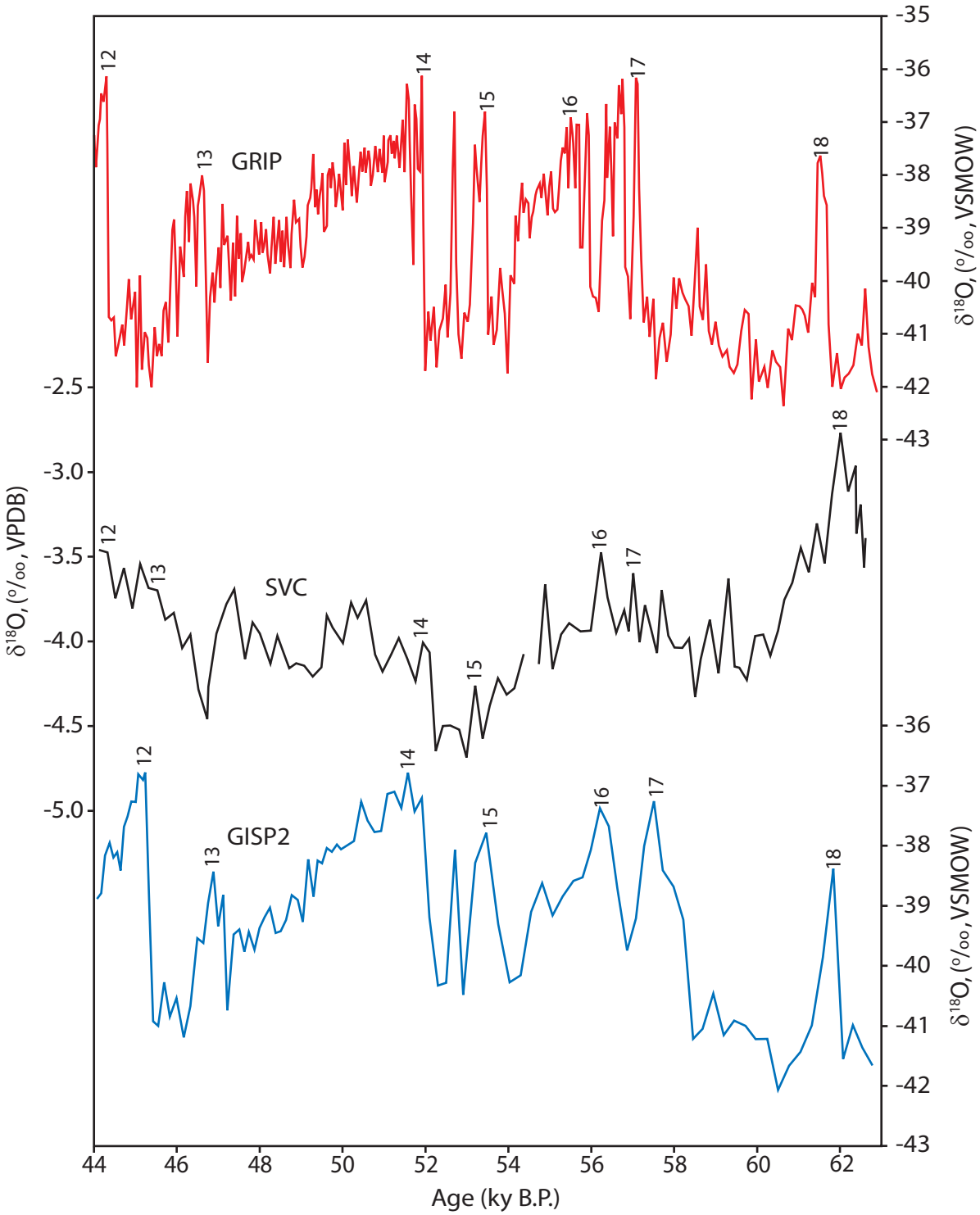

Figure 9. Spring Valley Caverns $\delta^{18}O$ record (SVC, black) compared to those from the Greenland Ice-core Project (GRIP, red) and Greenland Ice Sheet Project 2 (GISP2, blue). Dansgaard-Oeschger events are represented by whole numbers and are correlatable across the three records. GISP2 and GRIP data are available from the NOAA/NGDC Paleoclimatology Program, Boulder CO, USA website: http://www.ngdc.noaa.gov/paleo/paleo.hmtl.

which follow larger D-O events (Bond et al., 1993). By stopping regular patterns of NADW circulation, this injection of cold fresh water interrupts the northward conveyance of warm tropical water.

Global Climate Model (GCM) simulations carried out by Stocker (2000) predict that interruption of NADW circulation alters the relative strength of zonal and meridional atmospheric circulation cells affecting the mid-continent. Times of warmth in Greenland, corresponding to normal NADW circulation, are also times of dominant meridional atmospheric circulation in the northern hemisphere, and unimpeded northwards heat flow (Dorale and Edwards, 2000; Wang et al., 2001).

Times of reduced NADW circulation were periods dominated by zonal winds, carrying cold air from the arctic across the northern Atlantic and Europe (Dorale and Edwards, 2000). The mid-continental region also probably experienced cooling because of a drop in advected tropical heat due to weakening of the northward Hadley cell of the Intertropical Convergence Zone (Broccoli et al., 2006).

This reduction in advected heat resulted in colder temperatures at northern and middle latitudes. Thus the relative cold periods in the Spring Valley record from ~61-58 kyr and from ~54-51 kyr can be interpreted as having resulted from glacial melt in response to D-O events 18 and 16, respectively. This response may be the ~55 kyr event observed in the Spring Valley Caverns record, which was also noted by Dorale et al. (1998) in a record from Crevice Cave, Missouri. Conversely, the return to warmer temperatures observed in the Spring Valley record at ~52 ka may represent the reestablishment of typical NADW circulation, and thus the return to conditions which allowed the gradual buildup of Laurentide ice prior to the Last Glacial Maximum.

This model is supported by depositional evidence from the Roxana Silt, a widespread loess blown from glacial outwash plains beginning at ~55 ka, across the Upper Mississippi Valley (Leigh, 1994, Forman et al., 1992). In this scenario, loess deposition was driven by cool, dry, zonal atmospheric circulation corresponding to the cold period following the ~55 kyr event.

The occurrence of Spruce charcoal throughout the Roxana Silt in Wisconsin (Leigh, 1994) provides additional evidence from the SVC $\delta^{13}C$ curve for a conifer hardwood forest ecosystem overlying the cave site throughout deposition. Phases of relatively high $\delta^{13}C$ values (~-6.5 per mil) in the record generally occur at times of warmer temperature and may correspond to the contribution of some C_4 grasses.

CONCLUSIONS

The late Pleistocene isotope record from Spring Valley Caverns documents mid-continent climate change throughout the Mid-Wisconsinan interstadial. Correlation between the Spring Valley Record and other mid-continent records, as well as records from Greenland and China, indicate hemispheric wide control of climate patterns throughout the late Pleistocene. These correlations along with GCM models suggest that climate changes may be driven by disruptions to NADW thermohaline circulation. The ability to recognize these changes in oceanic circulation in the historic record will lead to a greater understanding of their ability to regulate climate.

ACKNOWLEDGEMENTS

First and foremost my thanks go out to Sushmita Dasgupta for all the guidance and good humor she has shown me throughout this process. Additional thanks go to Megan Kelly, Carolyn Dykowski, and Xienfang Wang for guidance and assistance throughout the Uranium Thorium dating process. I would also like to thank Carey Tinkelenburg and her housemates for all their hospitality during my weekend stays in Minneapolis. I am grateful to Larry Edwards and Calvin Alexander for their thoughtful input, and Clint Cowan, and Sarah Titus for their help throughout the writing process. I would also like to thank the cave owner, John Ackerman, for access to Spring Valley Caverns and to the stalagmite. Dan Costello and Ben Hardt assisted in sample collection. Thanks also to Dr. Yue-Gau Chen and Hong-Wei Chiang for carrying out the stable isotope analyses.

REFERENCES CITED

Alley, R. B., Meese, D. A., Shuman, C. A., Gow, A. J., Taylor, K. C., Grootes, P. M., White, J. W. C., Ram, M., Waddington, E. D., Mayewski, P. A., and Zielinski, G. A., 1993, Abrupt increase in Greenland snow accumulation at the end of the Younger Dryas event: Nature, v. 362, no. 6420, p. 527.

Atkinson, T. C., 1983, Growth mechanisms of speleothems in Castleguard Cave, Columbia Icefields, Alberta, Canada: Arctic and Alpine Research, v. 15, no. 4, p. 523-536.

Baker, R. G., Bettis, E. A., Denniston, R. F., Gonzalez, L. A., Strickland, L. E., and Krieg, J. R., 2002, Holocene paleoenvironments in southeastern Minnesota - chasing the prairie-forest ecotone: Palaeogeography, Palaeoclimatology, Palaeoecology, v. 177, no. 1-2, p. 103-122.

Bjork, S., Kromer, B., Johnsen, S., Bennike, O., Hammarlund, D., Lemdahl, G., Possnert, G., Rasmussen, T. L., Wohlfarth, B., Hammer, C. U., and Spurk, M., 1996, Synchronized terrestial-atmospheric deglacial records around the North Atlantic: Science, v. 274, p. 1155-1160.

Black, R. F., Goldthwait, R. P., and Willman, H. B., 1973, The Wisconsinan Stage: Boulder, CO, Geological Society of America.

Bond, G., Broecker, W., Johnsen, S., McManus, J., Labeyrie, L., Jouzel, J., and Bonani, G., 1993, Correlations between climate records from North Atlantic sediments and Greenland Ice: Nature, v. 365, no. 6442, p. 143.

Boutton, T. W., 1991, Stable Carbon Isotope Ratios of Natural Materials, *in* Coleman, D. C., and Fry, B., eds., Carbon Isotope Techniques: San Diego, Academic Press, p. 155-171.

Broccoli, A. J., Dahl, K. A., and Stouffer, R. J., 2006, Response of the ITCZ to northern hemisphere cooling: Geophysical Research Letters, v. 33, p. 1-4.

Broecker, W. S., 1994, Massive iceberg discharges as triggers for global climate change: Nature, v. 372, no. 6505, p. 421.

Dansgaard, W., 1964, Stable isotopes in precipitation: Tellus, v. 16, p. 436-468.

Denniston, R. F., González L. A., Baker R. G., Reagan M. K., Asmerom Y., Edwards R. L., and Alexander E. C., 1999, Speleothem evidence for Holocene fluctuations of the prairie-forest ecotone, north-central USA: Holocene, v. 9, no. 6, p. 671-676.

Dorale, J. A., and Edwards, R. L., 2000, A continuous 66-23 ka record of d18O variations from Crevice Cave, Missouri and the timing of Dansgaard-Oeschger and Heinrich Events: University of Minnesota.

Dorale, J. A., Edwards, R. L., Alexander, E. C., Shen, C. C., Richards, D. A., and Cheng, H., 2001, Uranium-series dating of speleothems; current techniques, limits and applications, *in* Mylroie, J., and Sasowsky, I. D., eds., Studies of Cave Sediments: New York, Kluwer Academic Plenum.

Dorale, J. A., Edwards, R. L., Ito, E., and Gonzalez, L. A., 1998, Climate and Vegetation History of the Midcontinent from 75 to 25 ka: A Speleothem Record from Crevice Cave, Missouri, USA: Science, v. 282, no. 5395, p. 1871-1874.

Dreimanis, A., and Goldthwait, R. P., 1973, Wisconsin Glaciation in the Huron, Erie, and Ontario Lobes, *in* Black, R. F., Goldthwait, R. P., and Willman, H. B., eds., The Wisconsinan Stage, Geological Society of America Memoir 136, p. 71-106.

Edwards, R. L., Chen, J. H., and Wasserburg, G. J., 1987, (super 238) U- (super 234) U- (super 230) Th- (super 232) Th systematics and the precise measurement of time over the past 500,000 years: Earth and Planetary Science Letters, v. 81, no. 2-3, p. 175-192.

Ford, D. C., Smart, P. L., and Ewers, R. O., 1983, The physiography and speleogenesis of Castleguard Cave, Columbia Icefields, Alberta, Canada: Arctic and Alpine Research, v. 15, no. 4, p. 437-450.

Ford, D. C., and Williams, P. W., 1989, Karst Geomorphology and Hydrology: London, United Kingdom (GBR), Unwin Hyman.

Forman, S. L., Bettis, E. A., III, Kemmis, T. J., and Miller, B. B., 1992, Chronologic evidence for multiple periods of loess deposition during the late Pleistocene in the Missouri and Mississippi River valley, United States; implications for the activity of the Laurentide ice sheet: Palaeogeography, Palaeoclimatology, Palaeoecology, v. 93, no. 1-2, p. 71-83.

Friedman, I., O'Neil, J. R., and Fleischer, M., 1977, Compilation of stable isotope fractionation factors of geochemical interest: United States Geological Survey Professional Paper P 0440-KK, 12 p.

Fry, J. C., and Willman, H. B., 1973, Wisconsinan Climatic History Interpreted from Lake Michigan Lobe Deposits and Soils, *in* Black, R. F., Goldthwait, R. P., and Willman, H. B., eds., The Wisconsinan Stage, Geological Society of America Memoir 136, p. 135-152.

Hedges, J., and Alexander, E. C., Jr., 1985, Karst-related features of the Upper Mississippi Valley region: Studies in Speleology, v. 6, p. 41-49.

Hendy, C. H., and Wilson, A. T., 1968, Paleoclimatic data from Speleothems: Nature, v. 216, p. 48-51.

Kaufman, A., and Broecker, W. S., 1965, Comparison of Th (super 230) and C (super 14) ages for carbonate materials from Lakes Lahontan and Bonneville: Journal of Geophysical Research, v. 70, no. 16, p. 4039-4054.

Kneller, M., and Peteet, D., 1999, Late-glacial to early Holocene climate changes from a Central Appalachian pollen and macrofossil record: Quaternary Research, v. 51, no. 2, p. 133-147.

Kral, Z., 1971, Studie vznika a barevnosti krapnikovych utvara: Ceskoslovensky Kras, v.23, p. 7-15

Langmuir, D., 1997, Aqueous environmental geochemistry: Upper Saddle River, Prentice Hall.

Langmuir, D., and Herman, J. S., 1980, The mobility of thorium in natural waters at low temperatures: Geochimica et Cosmochimica Acta, v. 44, no. 11, p. 1753-1766.

Leigh, D. S., and Knox, J. C., 1994, Loess of the Upper Mississippi Valley Driftless Area: Quaternary Research, v. 42, no. 1, p. 30-40.

Lively, R. S., 1983, Late Quaternary U-series speleothem growth record from southeastern Minnesota: Geology, v. 11, no. 5, p. 259-262.

Richards, D. A., and Dorale, J. A., 2003, Uranium-series chronology and environmental applications of speleothems: Reviews in Mineralogy and Geochemistry, v. 52, p. 407-460.

Runkel, A. C., Tipping R.G., Alexander, E. C., Green, J. A., Mossler, J. H., and Alexander, S. C., 2003, Hydrogeology of the Paleozoic bedrock in southeastern Minnesota: Minnesota Geological Survey Report of Investigations 61, 105 p., 2 pls.

Spotl, C., Mangini, A., Frank, N., Eichstadter, R., and Burns, S. J., 2002, Start of the last interglacial period at 135 ka: Evidence from a high Alpine speleothem: Geology, v. 30, no. 9, p. 815-818.

Stocker, T. F., 2000, Past and future reorganizations in the climate system: Quaternary Science Reviews: v. 19, no. 1-5, p. 301-319.

Wang, Y. J., Cheng, H., Edwards, R. L., An, Z. S., Wu, J. Y., Shen, C. C., and Dorale, J. A., 2001, A High-Resolution Absolute-Dated Late Pleistocene Monsoon Record from Hulu Cave, China: Science, v. 294, no. 5550, p. 2345-2348.

Winograd, I. J., Coplen, T. B., Landwehr, J. M., Riggs, A. C., Ludwig, K. R., Szabo, B. J., Kolesar, P. T., and Revesz, K. M., 1992, Continuous 500,000 year climate record from vein calcite in Devils Hole, Nevada: Science, v. 258, p. 255-260.

Yonge, C. J., Ford, D. C., Gray, J., and Schwarcz, H. P., 1985, Stable isotope studies of cave seepage water: Chemical Geology; Isotope Geoscience Section, v. 58, no. 1-2, p. 97-105.

Appendix 1. Stable Isotope Values for SVC-06
Analytical error is 0.08‰ (2σ)

Sample No.	Depth (mm)	Age (yr B.P.)	Intensity	STD (1σ)	δ13C	δ18O
SVC-06-01	6	44146	6933.698	0.021	-7.491667	-3.464667
SVC-06-02	8.2	44347	6432.561	0.022	-7.849667	-3.478667
SVC-06-03	10.4	44547	6305.107	0.019	-7.753667	-3.745667
SVC-06-04	12.6	44748	7452.778	0.023	-7.436667	-3.569667
SVC-06-05	14.8	44949	8539.021	0.023	-7.772667	-3.805667
SVC-06-06	17	45150	7749.408	0.02	-7.747667	-3.548667
SVC-06-07	19.2	45350	8673.501	0.02	-7.649667	-3.686667
SVC-06-08	21.4	45551	8502.835	0.018	-7.274667	-3.700667
SVC-06-09	23.6	45752	8053.392	0.012	-8.269667	-3.873667
SVC-06-10	25.8	45953	8603.749	0.009	-7.909667	-3.835667
SVC-06-11	28	46153	6275.468	0.023	-8.188667	-4.040667
SVC-06-12	30.2	46354	6188.697	0.023	-8.268667	-3.962667
SVC-06-13	32.4	46555	6720.056	0.037	-8.554667	-4.287667
SVC-06-14	34.6	46756	7161.004	0.025	-8.790667	-4.459667
SVC-06-15	35	46792	8658.029	0.006	-8.098667	-4.270667
SVC-06-16	37.2	46986	8713.631	0.015	-7.179667	-3.957667
SVC-06-17	40	47232	8603.067	0.019	-7.914667	-3.782667
SVC-06-18	42	47408	7183.805	0.02	-8.257667	-3.694667
SVC-06-19	45	47673	6156.956	0.012	-6.834667	-4.106667
SVC-06-20	47	47849	8434.757	0.019	-8.030667	-3.891667
SVC-06-21	49	48025	9040.955	0.018	-6.857667	-3.956667
SVC-06-22	52	48289	8596.969	0.014	-8.030667	-4.132667
SVC-06-23	53.8	48448	7886.306	0.013	-6.831667	-3.970667
SVC-06-24	57	48729	7515.608	0.011	-7.033667	-4.158667
SVC-06-25	59	48905	7623.933	0.016	-7.129667	-4.132667
SVC-06-26	61	49082	7866.672	0.015	-7.120667	-4.146667
SVC-06-27	63.5	49302	6850.352	0.025	-7.821667	-4.209667
SVC-06-28	66	49522	7336.97	0.025	-7.505667	-4.156667
SVC-06-29	67.5	49654	8569.655	0.014	-6.668667	-3.850667
SVC-06-30	69	49786	8361.211	0.017	-6.947667	-3.921667
SVC-06-31	76	50033	8559.378	0.02	-8.504667	-4.011667
SVC-06-32	81.5	50227	8543.902	0.012	-7.806667	-3.773667
SVC-06-33	86	50386	8275.643	0.014	-7.150667	-3.862667
SVC-06-34	92	50598	8400.223	0.022	-7.257667	-3.760667
SVC-06-35	98	50810	8683.18	0.031	-8.247667	-4.078667
SVC-06-36	104	50993	8777.979	0.015	-8.462667	-4.179667
SVC-06-37	111	51207	8425.897	0.015	-8.583667	-4.083667
SVC-06-38	117	51390	6859.889	0.017	-8.379667	-3.985667
SVC-06-39	123.5	51588	8081.512	0.024	-8.154667	-4.107667
SVC-06-40	130	51786	8624.387	0.012	-8.690667	-4.235667
SVC-06-41	137	51964	8615.164	0.015	-8.842667	-4.010667
SVC-06-42	143	52116	8559.048	0.018	-8.007667	-4.065667
SVC-06-43	149.5	52281	8115.355	0.024	-8.003667	-4.647667
SVC-06-44	156	52446	8575.599	0.022	-8.480667	-4.501667
SVC-06-45	163	52624	8320.491	0.026	-8.505667	-4.500667
SVC-06-46	170	52835	6176.851	0.028	-7.670667	-4.523667
SVC-06-47	176	53016	7510.245	0.016	-8.349667	-4.685667
SVC-06-48	182.5	53212	7884.675	0.012	-7.621667	-4.266667

Sample No.	Depth (mm)	Age (yr B.P.	Intensity	STD (1σ)	δ13C	δ18O
SVC-06-49	189	53408	6316.382	0.023	-7.783667	-4.574667
SVC-06-50	195	53589	8129.029	0.023	-7.708667	-4.382667
SVC-06-51	201	53770	7368.235	0.016	-7.504667	-4.222667
SVC-06-52	208	53981	8582.777	0.009	-7.311667	-4.315667
SVC-06-53	214.5	54177	6256.953	0.024	-6.504667	-4.280667
SVC-06-54	222	54403	8294.884	0.011	-6.724667	-4.078667
SVC-06-55	229	54614	8440.83	0.019	-5.757667	-2.572667
SVC-06-56	234	54765	8523.302	0.013	-7.674667	-4.134667
SVC-06-57	239	54916	8551.259	0.023	-6.643667	-3.667667
SVC-06-58	245	55097	8649.233	0.013	-7.564667	-4.162667
SVC-06-59	252	55308	8603.005	0.019	-6.454667	-3.961667
SVC-06-60	258	55489	8300.155	0.013	-6.807667	-3.897667
SVC-06-61	267	55760	8614.072	0.01	-7.145667	-3.943667
SVC-06-62	275	56018	8625.993	0.022	-8.155667	-3.940667
SVC-06-63	282.5	56259	8589.594	0.012	-7.008667	-3.478667
SVC-06-64	287.5	56421	7939.636	0.018	-7.786667	-3.744667
SVC-06-65	294	56630	8232.101	0.011	-8.375667	-3.950667
SVC-06-66	300	56823	8500.861	0.025	-7.543667	-3.819667
SVC-06-67	303	56920	6854.518	0.019	-7.768667	-3.940667
SVC-06-68	306	57038	8516.71	0.018	-7.791667	-3.600667
SVC-06-69	310	57196	8365.163	0.016	-8.152667	-4.005667
SVC-06-70	313	57315	8648.354	0.014	-7.389667	-3.789667
SVC-06-71	317	57472	8518.379	0.007	-8.815667	-3.929667
SVC-06-72	320.5	57610	8453.491	0.015	-8.681667	-4.068667
SVC-06-73	323.5	57729	6531.16	0.021	-8.336667	-3.699667
SVC-06-74	327.5	57887	8704.951	0.018	-7.825667	-3.968667
SVC-06-75	331	58025	8446.439	0.025	-7.079667	-4.038667
SVC-06-76	336	58222	8714.12	0.015	-6.705667	-4.043667
SVC-06-77	346	58385	8560.403	0.017	-7.917667	-3.987667
SVC-06-78	356	58547	8355.012	0.017	-7.818667	-4.330667
SVC-06-79	364	58677	7821.77	0.018	-7.847667	-4.107667
SVC-06-80	379	58891	8394.702	0.027	-7.636667	-3.874667
SVC-06-81	394	59105	8581.484	0.012	-7.109667	-4.188667
SVC-06-82	410	59334	8684.807	0.012	-7.457667	-3.629667
SVC-06-83	414	59485	8734.825	0.013	-7.901667	-4.148667
SVC-06-84	417	59599	8634.827	0.017	-6.510667	-4.157667
SVC-06-85	422	59788	8667.93	0.018	-7.376667	-4.228667
SVC-06-86	427	59977	8439.613	0.017	-6.702667	-3.970667
SVC-06-87	432	60166	8645.192	0.012	-7.325667	-3.964667
SVC-06-88	437	60355	7966.645	0.01	-7.709667	-4.086667
SVC-06-89	442	60544	7721.538	0.025	-7.656667	-3.939667
SVC-06-90	446	60695	8704.446	0.014	-7.923667	-3.757667
SVC-06-91	455	60887	7141.323	0.007	-7.061667	-3.658667
SVC-06-92	464	61079	8693.641	0.015	-7.651667	-3.449667
SVC-06-93	473	61270	6680.729	0.03	-7.743667	-3.592667
SVC-06-94	482	61462	8384.952	0.016	-7.834667	-3.308667
SVC-06-95	491	61654	9108.214	0.019	-8.462667	-3.541667
SVC-06-96	500	61846	8134.01	0.013	-7.003667	-3.134667
SVC-06-97	509	62038	8371.965	0.014	-6.575667	-2.771667
SVC-06-98	518	62230	8393.414	0.02	-7.785667	-3.114667

Sample No.	Depth (mm)	Age (yr B.P.	Intensity	STD (1σ)	δ13C	δ18O
SVC-06-99	526	62400	8121.111	0.025	-7.236667	-2.965667
SVC-06-100	531	62419	8695.574	0.012	-7.713667	-3.365667
SVC-06-101	556	62514	8112.189	0.015	-6.258667	-3.194667
SVC-06-102	581	62608	8361.449	0.018	-8.500667	-3.564667
SVC-06-103	588	62635	8495.039	0.009	-8.386667	-3.393667